Automatic Arterial Input Function Detection for Prostate Dynamic Contrast Enhanced MRI

Y. Zhu[1], M-C. Chang[2], F. M. Fennessy[3], and S. N. Gupta[4]
[1]Dept. of EECS, Syracuse University, Syracuse, NY, United States, [2]Vis. and Comp. Vision Lab, GE Global Research Center, Niskayuna, NY, United States, [3]Dept. of Radiology, Brigham and Women's Hospital, Boston, MA, United States, [4]Functional Imaging Lab, GE Global Research Center, Niskayuna, NY, United States

Introduction

Dynamic Contrast Enhanced MRI (DCEMRI) has shown promise in non-invasive assessment of tumor vascular properties with application in prostate cancer staging and treatment monitoring [1]. Accurate quantification from DCEMRI however, depends on the robust determination of the arterial input function (AIF) – concentration of contrast agent in feeding vasculature. Some pharmacokinetic models circumvent the problem of AIF by modeling the AIF or assuming it to be constant in all patient populations and basing them on blood sample measurements [2]. Data-driven AIF estimation can account for a patient-specific arterial input function and is therefore more quantitative. AIF is most routinely measured manually by the user selecting a region of interest in an appropriate vessel. These methods are time consuming and suffer from inter-subject variability. Therefore automated ways of estimating the AIF would be extremely desirable.

AIF determination in prostate DCEMRI is challenging because of extreme significant intensity non-uniformity due to the use of an endo-rectal coil. Therefore existing methods in the literature [3-4] do not perform well. In this work, we use both the temporal and spatial information of the dataset to determine the AIF for DCEMRI of the prostate. In order to address the problem of intensity non-uniformity in prostate datasets, we develop a Gamma variate function (GVF) fitting algorithm to find the pixels which have candidate shapes of AIF curves in time domain. The candidate pixels are then further refined using spatial information from the images to eliminate spurious pixels. We validate our method by clinical results and compare our automated AIF approach with expert user traced manual AIFs.

Methods

Acquisition: 8 patients with known prostate cancer were scanned on a 3T Signa HDX MRI scanner (GE Healthcare, Waukesha, WI) under IRB approved protocols, using a 3D SPGR sequence (TR/TE 3.8/1.3ms, FA 15°, BW ±31 kHz, FOV 26 cm, matrix 256 x 160 x 16, thickness 3 mm). In each study 50-65 volumes were obtained in 4-5 mins (~4.5 sec/volume). 0.1 mmol/kg Gd-DTPA was injected i.v at 0.3 cc/sec for 100 seconds (Figure 1a).

Manual AIF Selection: DICOM data was processed using a pharmacokinetic analysis package (Cinetool, GE Healthcare) custom built in IDL. Following inspection of the time series data, a small ROI was placed within the left femoral artery to generate the manual AIF. A central slice location was selected to minimize inflow effects. The generated signal-intensity curve was converted into [Gd] concentration estimates using a blood T1 value of 1.6s at 3T. The AIF curve was then scaled to peak concentration of 2.3 mM based on published data from model based AIFs [5] to make it robust to B1 inhomogeneity errors. Automatic delay correction was performed to shift the AIF so that the arrival of contrast matched that in the tumor for model-fitting.

Automatic AIF Estimation: In our method, we use GVF as a reference to detect the pixels which have characteristic shape of AIF using a fitting algorithm. After GVF fitting, the candidate pixels are further refined by applying spatial constraints by using a message passing algorithm to only select arterial pixels in close proximity so that they lie in a large vessel. We first derive theoretical bounds on GVF parameters that describe good AIF curves [6]. Next, for each pixel, the bolus arrival time and peak time are determined by calculating the curvature of the SI curve in time domain. Third, using these, a GVF is generated for each pixel. Fourth, based on the upper and lower bounds from our analytical methods, only the pixels whose parameters are within the range are selected as candidates to determine the AIF. Fifth, the spatial information of each pixel is applied into a message passing algorithm to find N *(=10)* pixels which have good fits with the GVF and minimize the distance to other candidate pixels. Finally, the AIF is determined by calculating the average signal curve from these N pixels and is scaled and delay-corrected similar to the manual AIF.

Results

Our method was tested on 8 clinical DCEMRI datasets. Fig. 1(a) shows an example DCEMRI image with the femoral artery ROI selected by the user as the manual AIF region. Fig. 1(b) shows the pixels selected by the automatic algorithm as candidate AIF pixels. Fig. 2 shows the automatic (red) and manual (blue) AIF in this example. The AIF curves obtained by the two methods were very well correlated as shown by the point-wise scatter plot in Fig. 3 (the colors represent each data set). The effect of using the automated AIF versus manual AIF on the estimation of pharmacokinetic maps using the general kinetic model was also analyzed. No significant difference was observed in all calculated PK maps. Sample K^{trans} parametric map from one dataset by using the manual AIF and the automatic AIF are shown in Figures. 4(a) and (b) respectively. The tumor in the right peripheral gland is clearly visualized in both cases (shown by arrow).

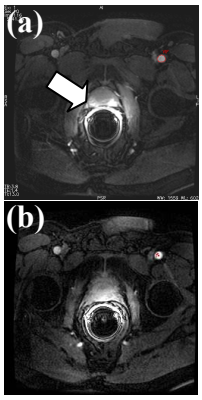

Figure 1

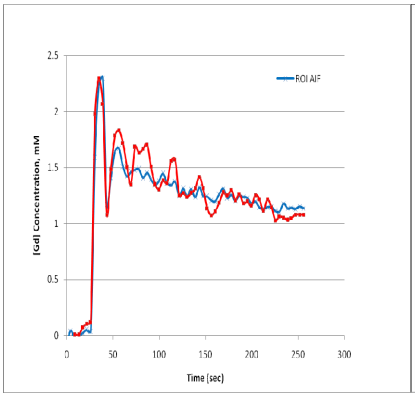

Figure 2

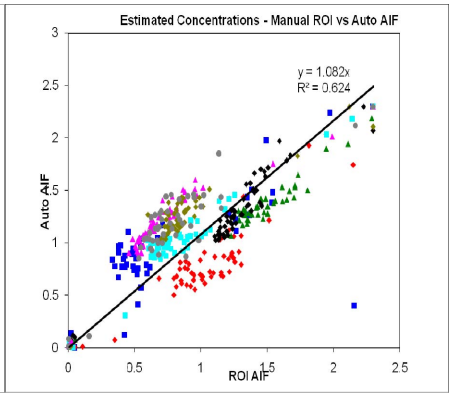

Figure 3

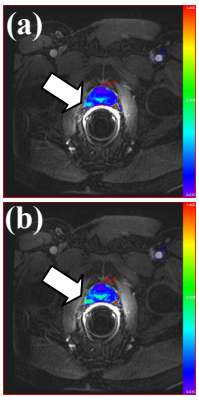

Figure 4

Conclusion

We have developed a fully automatic method to determine the AIF for prostate DCEMRI, and validated our method using clinical data. The method uses both temporal and spatial information and is robust to intensity non-uniformity in the prostate DCEMRI images. The analytically derived GVF parameter bounds significantly increase the accuracy and reduce the computation time. Our method is fully automatic without using any training data or prior information. Moreover, although our method is demonstrated for prostate DCEMRI, it is directly applicable to other body dynamic data.

References

[1] Hricak et al., *Radiology*:243(1):28-53; 2007.
[2] Morgan et al., *Br J Cancer*:94:1420-1427;2006.
[3] van Laarhoven et al., *JMRI*:18(3):315-20;2003.
[4] Mouridsen et al., *MRM*:55(3):524-31;2006.
[5] Priest et al., *MRM*:63:1044-1049;2010.
[6] Zhu et al., SPIE-MI 2011.

Acknowledgement of Support: This work was supported in part by Award Number U01CA151261 from the National Cancer Institute. The content is solely the responsibility of the authors and does not necessarily represent the official views of the National Cancer Institute or the National Institutes of Health.